AJNR

Functional MR of brain activity and perfusion in patients with chronic cortical stroke.

A G Sorensen, S H Wray, R M Weisskoff, J L Boxerman, T L Davis, F Caramia, K K Kwong, C E Stern, J R Baker and H Breiter

AJNR Am J Neuroradiol 1995, 16 (9) 1753-1762
http://www.ajnr.org/content/16/9/1753

Functional MR of Brain Activity and Perfusion in Patients with Chronic Cortical Stroke

A. G. Sorensen, S. H. Wray, R. M. Weisskoff, J. L. Boxerman, T. L. Davis, F. Caramia, K. K. Kwong, C. E. Stern, J. R. Baker, H. Breiter, I. E. Gazit, J. W. Belliveau, T. J. Brady, and B. R. Rosen

PURPOSE: (*1*) To determine whether functional MR can reliably map functional deficits in patients with stroke in the primary visual cortex; (*2*) to determine whether functional MR can reliably map perfusion deficits; and (*3*) to determine whether functional MR can give any additional diagnostic information beyond conventional MR. **METHODS:** Seven patients who had had a stroke in their primary visual system were examined using two functional MR techniques: (*1*) dynamic susceptibility contrast imaging, and (*2*) cortical activation mapping during full-field visual stimulation. Maps of relative cerebral blood volume and activation were created and compared with visual field examinations and conventional T2-weighted images on a quadrant-by-quadrant basis in five of these patients. **RESULTS:** Visual field mapping matched with both T2-weighted conventional images and activation mapping of 16 of 18 quadrants. In two quadrants, the activation maps detected abnormalities that were present on the visual field examination but not present on the T2-weighted images nor on the relative cerebral blood volume maps, which may indicate abnormal function without frank infarction. In addition, the activation maps demonstrated decreased activation in extrastriate cortex and had normal T2 signal and relative cerebral blood volume but was adjacent to infarcted primary cortex, mapping in vivo how stroke in one location can affect the function of distant tissue. **CONCLUSION:** Functional MR techniques can accurately map functional and perfusion deficits and thereby provide additional clinically useful information. Additional studies will be needed to determine the prognostic utility of functional MR in stroke patients.

Index terms: Brain, infarction; Magnetic resonance, functional

AJNR Am J Neuroradiol 16:1753–1762, October 1995

Functional magnetic resonance (MR) uses MR to investigate brain physiology. One type of functional MR, activation mapping, can show signal changes attributable to brain activity. Another type of functional MR also has been widely used: dynamic susceptibility contrast imaging, also known as relative cerebral blood volume mapping. We sought to investigate these two techniques in patients presenting with stroke in the visual system. Our goals were first, to validate the accuracy of functional MR and second, to determine the potential usefulness of functional MR in patients recovering from stroke.

The accuracy of functional MR still is being tested. Although functional MR is now in wide use, some investigators have felt that the patterns of activation seen were artifactual in nature, attributable to patient motion or other systematic error. We sought a patient population in which these questions of accuracy could be answered. We chose patients who had visual field defects caused by stroke. Because these patients have well understood functional neuroanatomy (1), their clinical ophthalmologic exam should directly correlate with the areas of activation as seen by functional MR. In addition,

Received December 2, 1994; accepted after revision May 16, 1995.

Supported in part by the Radiological Society of North America Research and Education Fund and National Public Health Service grants RO1-HL39810, RO1-CA40303, and PO1-CA48729.

Dr Sorensen received the Cornelius G. Dyke Memorial Award for this paper at the annual meeting of the American Society of Neuroradiology, Nashville, Tenn, 1994.

From the Department of Radiology and MGH-NMR Center (A.G.S., R.M.W., J.L.B., T.L.D., F.C., K.K.K., E.S., J.R.B., H.B., I.E.G., J.W.B., T.J.B., B.R.R.) and the Unit for Neurovisual Disorders (S.H.W.), Massachusetts General Hospital, Boston.

Address reprint requests to A. Gregory Sorensen, MD, Gray 2 Neuroradiology, Massachusetts General Hospital, Boston, MA 02114.

AJNR 16:1753–1762, Oct 1995 0195-6108/95/1609–1753

by studying these stroke patients, we hoped to gain insight into the potential utility of using functional MR to study the physiology of the brain after stroke. Stroke patients are at risk for recurrent stroke; approximately one quarter of stroke patients hospitalized annually for stroke have recurrent disease (2). Stroke often recurs in the same vascular territory (3); such patients may have a fixed perfusion deficit after their initial stroke. MR angiography has provided a noninvasive technique to evaluate arterial disease in these patients; however, the prognostic significance of large vessel disease is not always clear, particularly in the presence of collateral flow. Information regarding capillary-level hemodynamics may be synergistic or superior to MR angiography because of the variability of arterial supply.

Insight into these two problems (clinical-imaging correlation and the vascular substrate) would help with a third important question, that of stroke recovery. A variety of mechanisms have been proposed for stroke recovery (4), which basically break down into either local recovery mechanisms or distant recruitment mechanisms. Design of rational stroke recovery therapy will require elucidation of these mechanisms, particularly distinguishing between local recovery versus distant recruitment.

We used functional MR to investigate three questions: Can functional MR reliably map functional deficits? Can functional MR identify fixed hemodynamic defects or provide insight into the mechanism of functional deficits after stroke, even after the acute phase? Does functional MR in stroke patients yield any additional information beyond conventional MR?

To investigate these questions, we used two functional neuroimaging techniques in patients who had suffered a stroke in the primary visual system. We used task-activation mapping functional MR, which uses a "BOLD" (for blood oxygenation level dependent) (5, 6) contrast mechanism to evaluate underlying neuronal function indirectly. We also used dynamic contrast susceptibility imaging to evaluate relative cerebral blood volume (7, 8) (Belliveau J, Rosen B, Buxton R, et al, "Dynamic Imaging with Gadolinium of Magnetic Susceptibility Contract Effects in Experimental Brain Ischemia," presented at the Society for Magnetic Resonance in Medicine, Sixth Annual Meeting, 1987).

Materials and Methods

Patient Selection

Seven patients, 31 to 84 years of age, with either homonymous hemianopia or quadrantanopia, were each imaged using two functional imaging techniques; two of these patients were unable to cooperate well enough to allow useful data collection, leaving a total of five patients for data analysis. Our protocol was approved by our hospital's subcommittee on human studies, and all patients gave informed consent. The average time from onset of symptoms was 60 weeks (range, 4 to 185 weeks). Complete Goldman perimeter mapping or other standard visual field examination was available in all but one patient; where multiple visual field exams were available, the exam closest to the time of imaging were used.

Data Acquisition

The two functional MR techniques used echo-planar MR imaging, using a 1.5-T General Electric Signa (Milwaukee, Wis) MR scanner retrofitted with echo-planar imaging hardware from Advanced NMR Systems (Wilmington, Mass). All images were obtained using a 5-in surface coil placed over the occiput. In addition, all functional MR images were obtained along or parallel to the calcarine fissure (see Fig 1).

Our noncontrast technique consisted of a series of multisection gradient-echo images or asymmetric spin-echo images (9, 10), typically three or five 128 × 64 sections, 7-mm-thick sections with 0-mm gap. Photic stimulation was performed using light proof full-field photic stimulation goggles (model S10VS, Grass, Quincy, Mass) operating at 8 Hz. For gradient-echo imaging we used the fol-

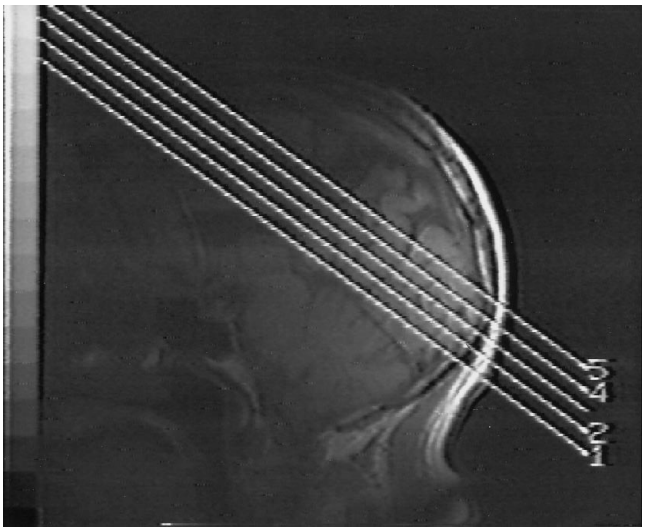

Fig 1. Scout image for section plane selection. Three or five oblique axial images were obtained parallel to the calcarine fissure. Both perfusion and activation maps were obtained along these section planes. We typically used 7-mm skip 0 section thickness.

lowing parameters: 1000 or 2000/50 (repetition time/echo time), and 90° flip angle. For asymmetric spin-echo images, parameters were 2000/75, with the 180° pulse offset by 25 milliseconds. All images were single shot (1 excitation). Patients were imaged in 60 seconds of darkness, followed by photic stimulation (goggle LEDs on) for 30 seconds, 30 seconds in darkness, 30 seconds of stimulation, and 30 seconds of darkness. Imaging time was 108 seconds. This imaging sequence was repeated once.

Our contrast technique consisted of rapid MR imaging after the intravenous injection of a bolus of 0.1 mmol/L gadopentetate dimeglumine, gadodiamide, or gadoteridol, using a prototype MR-compatible power injector (Medrad, Pittsburgh, Pa) to inject at 5 mL/s. Data are acquired for 20 seconds before beginning the injection to allow computation of a baseline for each voxel. One patient received 0.2 mM/kg of contrast (patient E.D.). A 256 × 128 single-shot echo-planar spin-echo image was obtained at each section with a single radio frequency excitation every 1500 milliseconds, with an echo time of 100 milliseconds, using a 7-mm section with 1.5 × 1.5-mm in-plane resolution and no intersection gap. Forty-five images at each section were obtained in 82 seconds. The patients were in darkness before and during this sequence. T2-weighted images were obtained in the same plane using a high-resolution spin-echo single-shot echo-planar sequence (2000/100), with matrix of 256 × 128. All echo-planar images were acquired with a 40 × 20-cm field of view.

Data Analysis

All images were transferred to computer work stations for further analysis on a voxel-by-voxel basis. We used Sun work stations (various models of SparcStations) and a Silicon Graphics minisupercomputer (model 4D 480/VGX) as well as custom-developed software for analyzing the contrast and noncontrast data and viewing the raw and computed images.

The noncontrast images were processed by grouping signal values for a voxel into either test group (during stimulation) or a control group (during darkness), and then applying Student's *t* test. This yields a map of probabilities (*P* values) for each voxel. After thresholding for a minimum *P* value (eg, $P = .01$), the activation maps were displayed on top of the T2-weighted raw images. The echo-planar spin-echo images were used as the underlying images to reduce image distortion when overlaying the activation maps on the anatomic images. Although the question of which statistical technique to use is not resolved and the details of this debate are beyond the scope of this article, we also used a Bonferroni correction technique to correct for performing multiple significance tests (11). This correction reduced the area of activation as expected but does not affect the findings in these patients.

The data from each contrast experiment was converted into a voxel-by-voxel map of relative cerebral blood volume according to a standard technique (12). This converts the change in signal as the single bolus of gadolinium contrast agent first passes through the brain microvasculature into a ΔR2 (where R2 = 1/T2) function and then a map of relative cerebral blood volume. Later in the study, we developed additional analysis techniques based on numerical and gamma fitting and applied them to the patient who received 0.2 mM/kg of contrast. This technique consists of fitting the ΔR2 function, S(t), to an equation of the form

$$S(t) = A^*(t - t_0)^{\alpha} * e^{(t-t_0)/\beta}.$$

This models the signal change caused by the bolus by a gamma function with parameters A, α, β, and t_0 (13). We created voxel-by-voxel maps of additional hemodynamic parameters including contrast bolus arrival time, peak signal change attributable to the bolus, the time of this peak signal change relative to the start of image acquisition, and estimates of the transit time such as the curve's full width at half maximum at each voxel.

One observer independently evaluated functional, relative cerebral blood volume, and conventional images for abnormal signal that would indicate stroke. Each patient's visual cortex was divided into four quadrants, using the calcarine fissure and the interhemispheric fissure as dividing lines. A quadrant was scored as abnormal if signal was partially or completely abnormal within it. Correlation between scores for each quadrant was made using conventional T2-weighted images, activation maps, cerebral blood volume maps, and the visual field examinations. Correlations were based on the known retinotopic mapping of the visual cortex (eg, the right upper visual field maps to the lower left visual cortex) (1). Where data were unavailable, correlations were not performed nor included in summary data.

Results

Two of the seven patients moved excessively during the functional portions of the exam (both male, 31 and 63 years of age). Our algorithms do not yet fully compensate for motion artifact and, as a result, both contrast and noncontrast mapping techniques yield spurious results in the presence of motion. Therefore, we excluded the data from these two patients from further analysis. Table 1 and Table 2 list the results for the remaining five patients' 20 quadrants.

Visual field analysis was unavailable in two quadrants. Activation maps, T2-weighted images, and relative cerebral blood volume maps all agree with the visual field examinations in more than 85% of the remaining quadrants. The activation maps agreed best (18 of 18 quadrants). Patients with hemianopia showed markedly asymmetric activation in the appropriate manner, according to the known retinotopic organization of the primary and secondary visual cortex. Figure 2 shows a typical patient with a

TABLE 1: Correlation of visual field exam with imaging modalities

Patient	Age, y	Stroke age, wk	Right Upper Visual Field				Right Lower Visual Field				Left Upper Visual Field				Left Lower Visual Field			
			Visual field exam	T2-weighted MR	Activation map	Relative cerebral blood volume	Visual field exam	T2-weighted MR	Activation map	Relative cerebral blood volume	Visual field exam	T2-weighted MR	Activation map	Relative cerebral blood volume	Visual field exam	T2-weighted MR	Activation map	Relative cerebral blood volume
B.C.	49	3	Abnormal	Abnormal	Abnormal	. . .	Abnormal	Abnormal	Abnormal	. . .	Normal	Normal	Normal	Normal	Normal	Normal	Normal	Normal
E.D.	75	17	Abnormal	Abnormal	Abnormal	Abnormal	Abnormal	Abnormal	Abnormal	Abnormal	Normal	Normal	Normal	Normal	**Abnormal**	**Normal**	**Abnormal**	**Normal**
E.L.	69	6	Normal	Normal	Normal	. . .	Abnormal	Abnormal	Abnormal	Abnormal	Normal	Normal	Normal	Normal	Normal	Normal	Normal	Normal
H.C.	59	91	Abnormal	Abnormal	Abnormal	Abnormal	**Abnormal**	**Normal**	**Abnormal**	**Normal**	Normal	Normal	Normal	Normal	Normal	Normal	Normal	Normal
B.B.	84	84	. . .	Normal	Normal	Normal	. . .	Abnormal	Abnormal	Abnormal	Normal	Normal	Normal	Normal	Normal	Normal	Normal	Normal

Note.—Abnormal indicates lesion present; normal, lesion absent. Visual field quadrants are referenced according to standard ophthalmalogic terminology, and all other results are referenced to these fields. Hence, the anatomic right lower quadrant on T2-weighted conventional MR imaging receives its main input from the left upper visual field. Quadrants where a mismatch exists in bold.

TABLE 2: Agreement of visual field exam with various MR techniques

Visual field exam vs activation maps	18 of 18	(100%)
Visual field exam vs T2-weighted images	16 of 18	(89%)
Visual field exams vs regional cerebral blood flow volume	13 of 15	(87%)
T2-weighted vs activation maps	18 of 20	(90%)

right homonymous hemianopia, with sparing of the central foveal region. In this patient, the relative cerebral blood volume, activation maps, and conventional T2-weighted images all corresponded to the visual field exam.

There was general agreement between abnormalities on the T2-weighted images and defects in the activation maps in the primary visual quadrants (16 of 18). However, in each patient, there was marked asymmetry of activation maps outside the primary visual cortex as well, where there was no abnormal T2 signal. Each patient showed activity outside the primary visual cortex (ie, in extrastriate cortex) on the unaffected side, but markedly decreased extrastriate activity on the affected side. Figure 2 demonstrates this finding as well.

In two quadrants of 18, there was normal signal on the T2-weighted images despite an abnormal visual field examination. In both of these quadrants, there was partial absence of vision. In these same two quadrants, however, there was abnormal activation but normal relative cerebral blood volume. Activation mapping, therefore, detected abnormalities of visual function in these two quadrants, which conventional imaging failed to demonstrate. Figure 3 illustrates this mismatch. Patient E.D. has a full or partial defect in three quadrants. Activation is absent from all three corresponding quadrants. Abnormal T2 signal is present only in two. The asymmetric activation is present even after Bonferroni statistical correction. Possible reasons for this finding are discussed below.

Contrast imaging produced confirmatory as well as unexpected findings. Patients who received 0.1 mM/kg of contrast agent showed on average only 10% signal drop in gray matter using our spin-echo technique. This change in signal produced relative cerebral blood volume maps with relatively poor signal-to-noise ratios. This led to nondiagnostic information in three quadrants and also to a modification in our technique (we now use 0.2 mM/kg routinely).

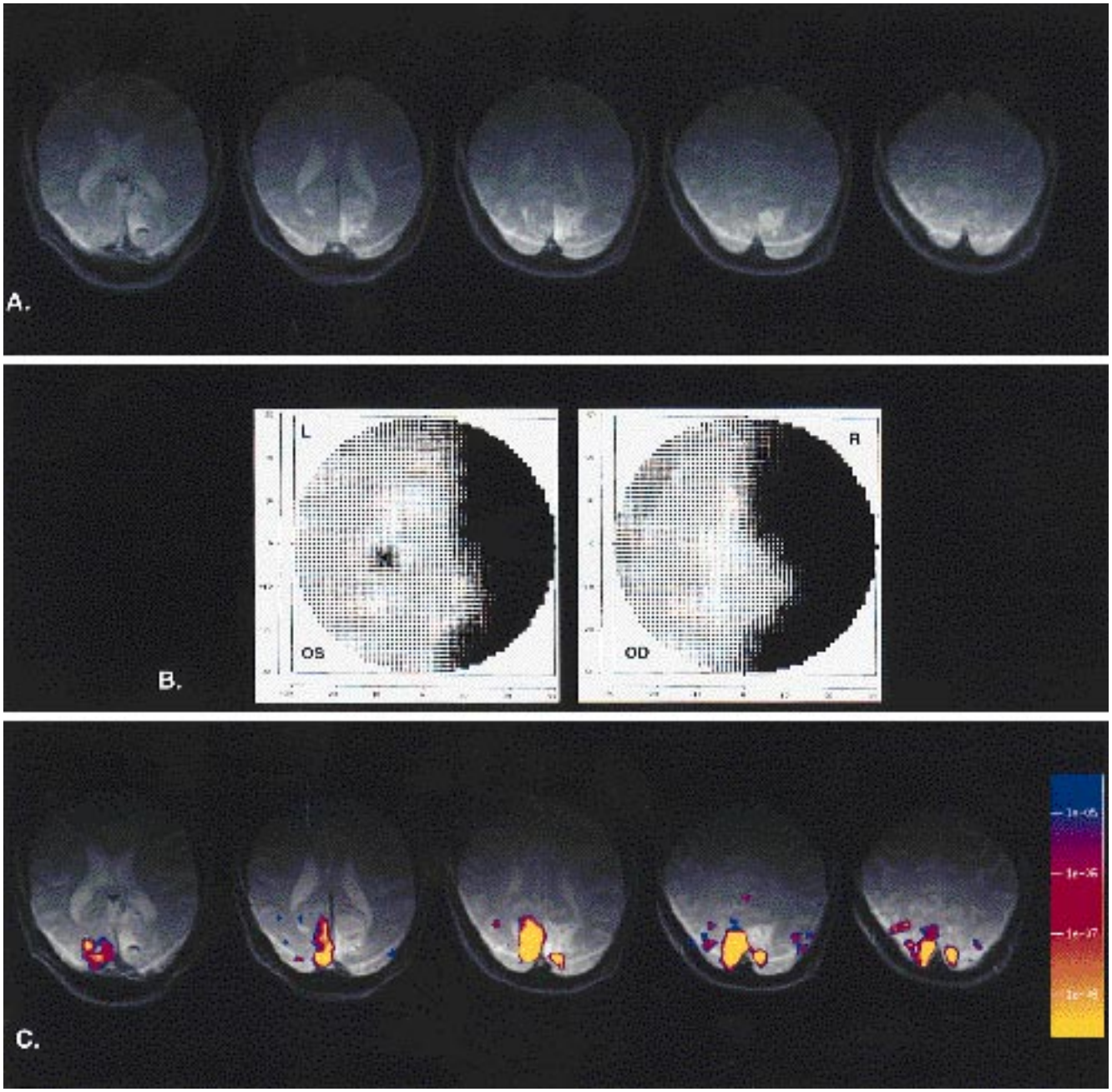

Fig 2. Activation mapping in a 49-year-old man, 6 weeks after he presented with a right homonymous hemianopia (patient E.L.).

A, Echo-planar T2-weighted spin-echo images parallel to the calcarine fissure. The center section is on the calcarine fissure itself.

B, Visual field maps, presented in standard ophthalmologic orientation, with the right visual field on the right.

C, Functional overlay. Overlaid on the T2-weighted images are the *t* test results in color from full-field photic stimulation during activation mapping. The color scale corresponds to the *P* value from the *t* test (eg, 1E-02 for $P = .01$; 1E-05 for $P = .00001$, etc). Images are presented in standard tomographic orientation. There is concordance between the activation mapping, which shows activity in the right primary visual cortex, corresponding to the normal left visual field. The left visual cortex shows a small focus of activation corresponding to the sparing of the fovea, with T2 bright signal in the remaining primary visual cortex. The extrastriate areas, however, are asymmetrically affected despite no abnormality on the underlying T2-weighted images, implying connectivity between the site of infarcted tissue in primary visual cortex and nearby uninfarcted tissue.

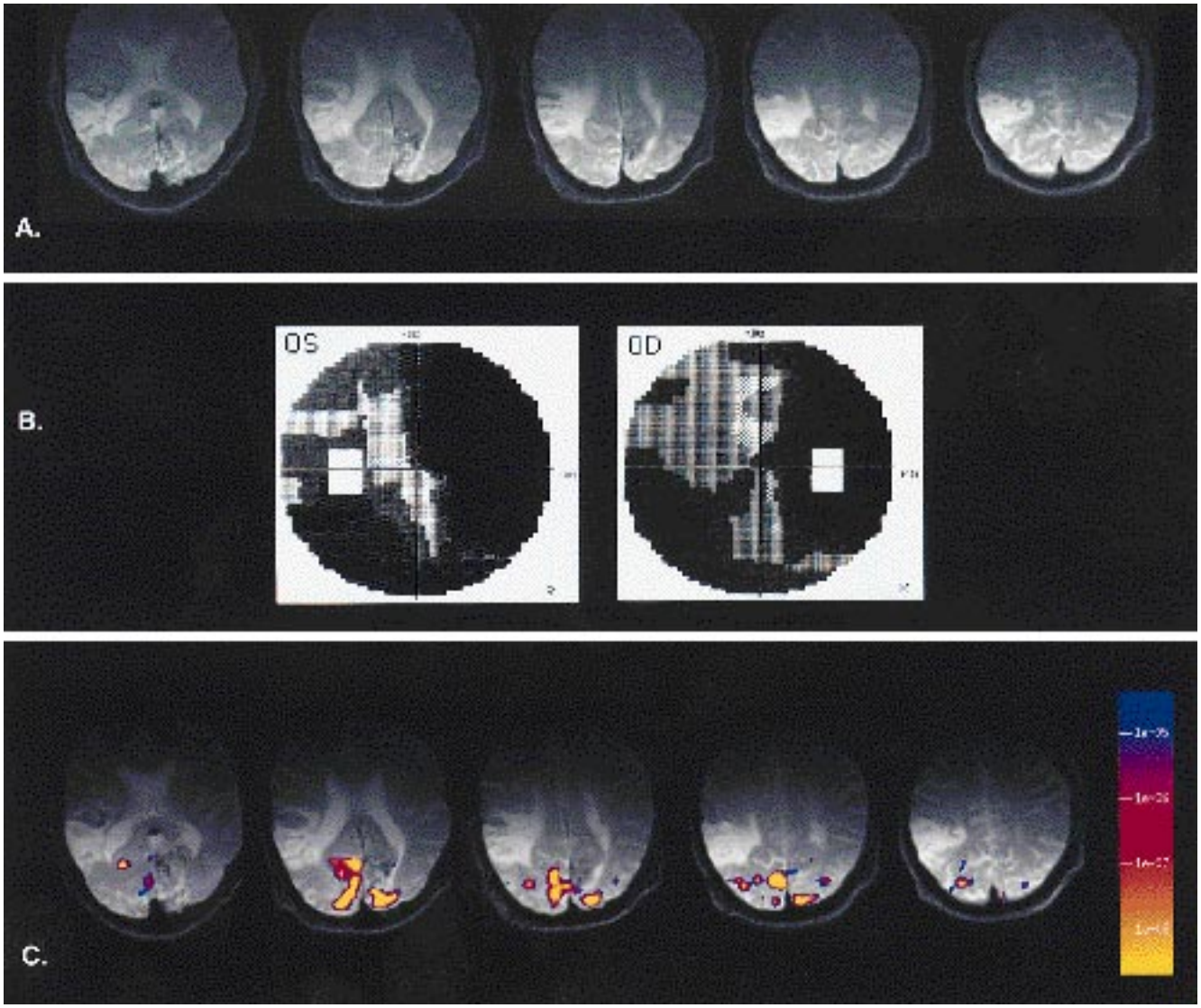

Fig 3. Activation mapping in a 75-year-old man 17 weeks after a left occipital infarct that was followed 2 weeks later by a second infarct in the right parietal lobe; visual exam showed right homonymous hemianopia and left inferior quandrantanopia (patient E.D.).

A, T2-weighted spin-echo echo-planar images parallel to the calcarine fissure, with the center section on the calcarine fissure.

B, Visual field maps showing absent vision in the right hemifield and a partial defect in the left lower quadrant.

C, Functional overlay. Overlaid on the T2-weighted images are the *t* test results in color from full-field photic stimulation during activation mapping, as in Figure 2. There is robust activity in the right lower occipital lobe, consistent with the one completely normal visual field quadrant. There is reduced activation in both the upper and lower left occipital lobes as well as in the upper right occipital lobe, consistent with the visual field map defects. However, T2 signal abnormality is not present in the upper right occipital lobe despite the decreased activation and abnormal visual field map. This is, therefore, a mismatch between the activation map and the T2-weighted images.

Patient E.D. received 0.2 mM/kg of gadolinium-based contrast agent and showed a 20% signal drop during the passage of the bolus of contrast through the brain vasculature; this produced better quality relative cerebral blood volume maps and also allowed creation of maps of other hemodynamic parameters. These maps are shown in Figure 4. Patient E.D. has two areas of abnormal signal on T2-weighted images consistent with infarct; only the left occipital lesion is in visual cortex. Both of these areas correspond to low relative cerebral blood volume, consistent with infarct. Also localized to the region of infarct is a localized decrease in peak signal drop (or peak $\Delta R2$), local increase in time to peak signal drop (the increase in time to peak is shown in the images as an increased signal intensity), and heterogeneous changes in

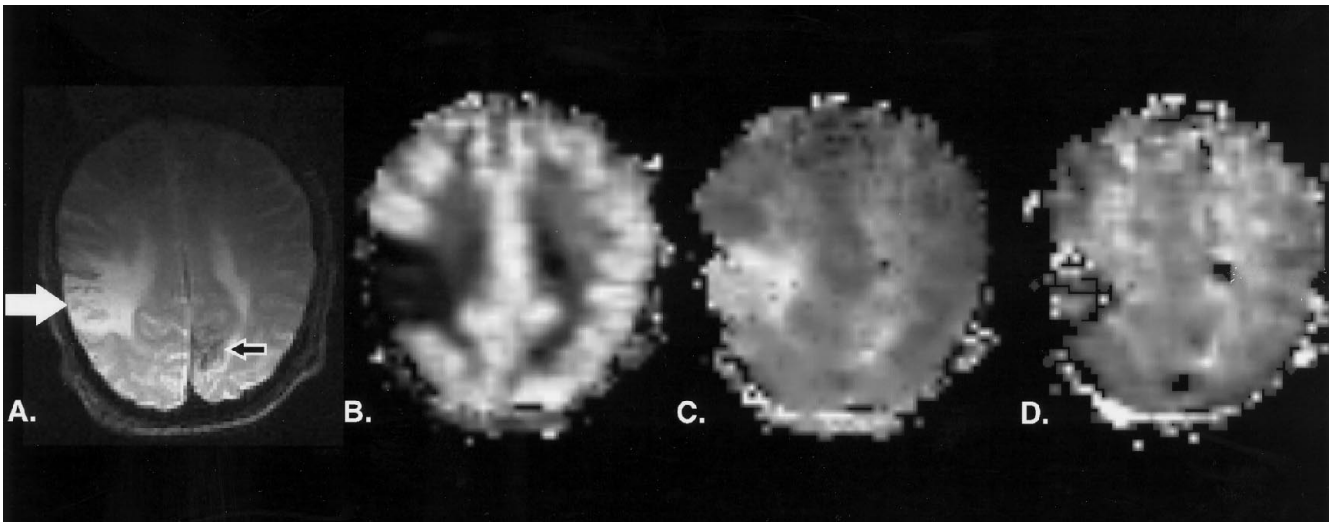

Fig 4. Perfusion mapping in the same patient at Figure 3, at the center section.

A, T2-weighted images. *Arrows* point to two infarcts.

B, Map of relative cerebral blood volume.

C, Map of peak signal change (ΔR2); the gray scale represents time in seconds from the start of imaging to peak ΔR2, where longer times are higher signal intensity.

D, Map of the full width of the signal change curve at half its maximum. All maps were obtained via numeric and gamma fitting as explained in the text, from a single bolus of 0.2 mM/kg of gadopenetate dimeglumine. The two infarcts have decreased relative cerebral blood volume and decreased peak ΔR2. There is a longer time to peak in the right parietal infarct, which is displayed as a brighter intensity; there is too little signal for the algorithm to determine times in the left occipital infarct, and those voxels are left black. There is heterogeneous but ill-defined change on the full width of the signal change curve at half its maximum maps. Note the subtle difference between the left and right hemispheres on the time to peak maps outside the areas of infarct.

transit times as shown on the images of the "full width at half maximum" parameter (*full width at half maximum* is one approximation to a mean transit time). Of particular note is the subtle but definite hemispheric asymmetry of the map of time to peak signal drop. The raw data for this are shown in more detail in Figure 5, The patient's right hemisphere (the side of the larger infarct) is slightly brighter than the left, indicating a longer time until the bolus of contrast reaches it; the delay within the area of probable gliosis is more than 5 seconds, but even outside the area of infarct there is more than 1 second of difference in the time to peak signal drop. Differences are not seen normally, based on our experience with some 200 patients undergoing relative cerebral blood volume mapping for reasons other than ischemic disease (unpublished observations, 1994).

Discussion

Our results indicate the ability of functional MR to map deficits after stroke. Not only did functional MR match all visual defects, it matched them even when conventional imaging missed the defects. In addition, activation mapping found additional areas of dysfunction outside the primary visual field quadrants, in areas known to be involved in higher-order visual processing. Conventional imaging provided no information about dysfunction in secondary cortical processing areas.

What is the explanation for the lack of functioning tissue outside the region of affected tissue as defined by conventional (anatomic) MR? Decreased function in secondary areas (eg, extrastriate cortex) is to be expected, given the known hierarchical organization of the visual system. Initial visual input travels first to the striate cortex along the banks of the calcarine fissure and from there to higher-order visual processing. Hence, a stroke in the primary visual cortex might decrease function in these higher centers. This study confirms in vivo that this indeed is the case—stroke in one area can affect not only immediately adjacent areas that appear normal on conventional imaging, but more distant areas, in this case, many centimeters away. This finding may be similar to what is sometimes called diaschisis (14). Our data indicate that diaschisislike lesions may not be detectable by conventional MR but can by func-

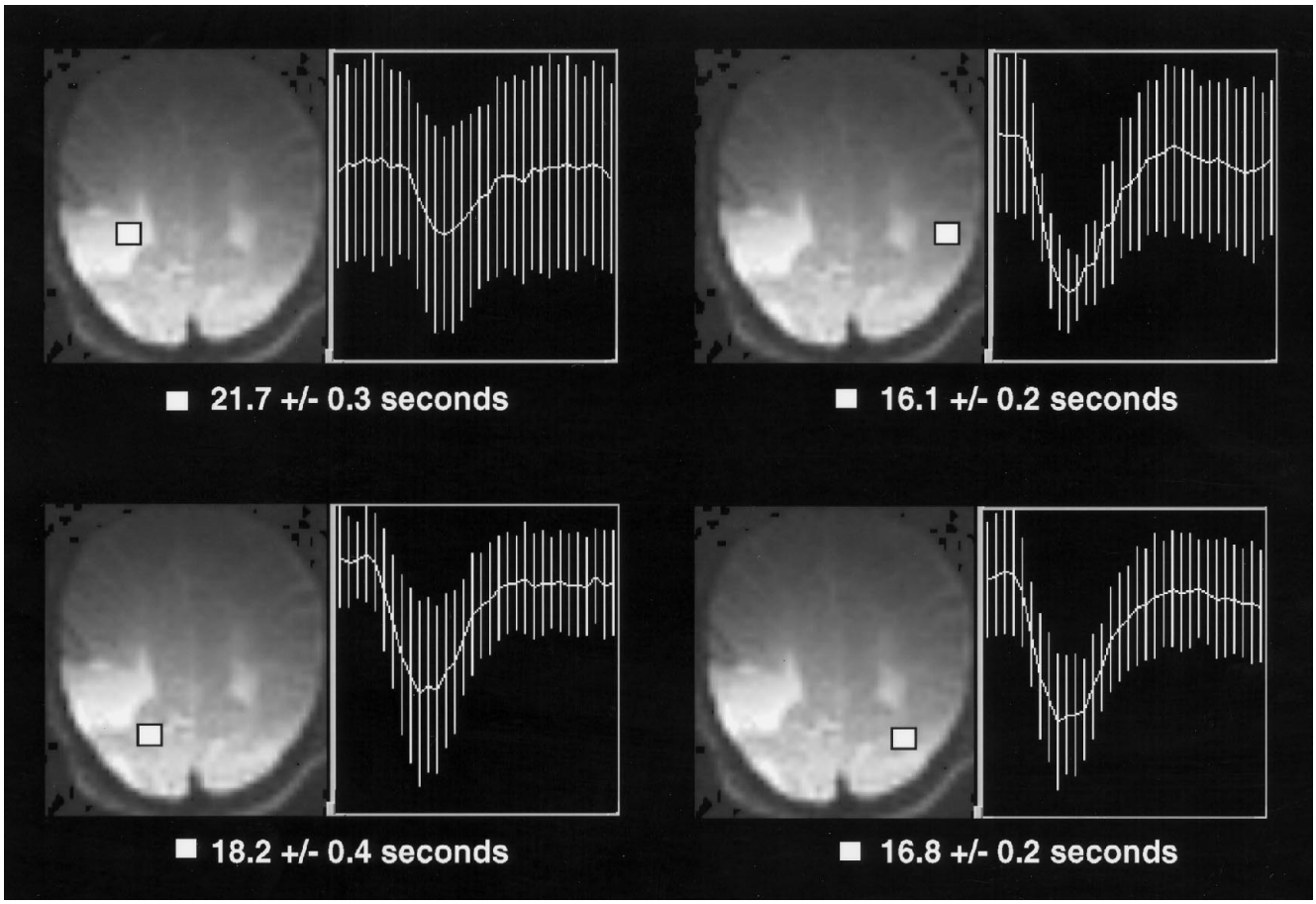

Fig 5. Detail and analysis from the time to peak ΔR2 maps from Figure 4 (patient E.D.), fourth highest section. Four regions of interest are displayed over the original echo-planar images, with their corresponding mean signal versus time curves from which the maps were generated (the vertical bars at each time point represent the standard deviation of the region of interest; all curves are on the same scale, but signal intensity values are arbitrary). Only the portion of the curve that corresponds to the passage of contrast is shown. The calculated time to peak ΔR2 for these regions of interest is also displayed. The values are in seconds from the end of the 8-second bolus injection of contrast. There is more than 5 seconds of delay between the normal left hemisphere tissue and the infarcted tissue at the same level. This is consistent with delayed perfusion through this region. Note also, however, that in the right hemisphere, there is a nearly 1½-second delay in peak signal change when compared with the opposite side. There is no asymmetry to relative cerebral blood volume nor peak ΔR2, implying this is not ischemia, but delayed perfusion.

tional MR techniques. This suggests that functional MR techniques can be applied to the understanding of stroke and recovery by serial examination of damaged cortex, work that we are undertaking.

Perhaps more challenging is understanding the lack of activity in primary visual cortex where there is no abnormal T2 signal. What is the reason for the mismatch between the areas of T2 abnormality and activation in these areas? There are a number of possible explanations. First, the neuronal input may never make it to primary visual cortex; the patient could have had damage to optic radiations such as Meyer loop, damage to the lateral geniculate nucleus, or at least in theory, bilateral retinal damage. This was at least partly the case for the patient shown in Figure 3, in whom a large middle cerebral artery territory infarct damaged at least a portion of Meyer's loop. A second possibility is that the abnormal activation maps could represent damage of enough neurons to decrease function but not enough to cause frank necrosis visible on T2-weighted imaging.

A third, and much more speculative, possibility for a portion of the mismatch between activation and T2 abnormality is that the neurons may be nonfunctioning but not infarcted. Our data may support such a speculation; in particular, the dynamic contrast imaging plays a helpful role. In the two quadrants where decreased activation but normal T2 signal was

present, there was normal relative cerebral blood volume. Hence, there are two studies—the activation studies and the visual field examinations—that imply that there are damaged neurons in these quadrants, but two studies (conventional MR and relative cerebral blood volume) that indicate no frank infarction, analagous perhaps to what has been termed "hibernating myocardium" in the heart (15). Further support for our speculation is found in the mismatch between function and T2/relative cerebral blood volume in patient E.D.; this mismatch is in the right upper hemisphere, the same location where Figures 4 and 5 imply there is delayed passage of contrast and where Meyer's loop fibers are less likely to be the primary input. More sophisticated techniques, such as extracting true cerebral blood flow information, will be needed to support these speculative hypotheses.

Figures 4 and 5 demonstrate that susceptibility-contrast MR can fulfill in part a second goal of this study: to demonstrate the ability of MR to provide local hemodynamic information. Additional investigation is needed to determine which of these hemodynamic parameters, if any, have prognostic implications, and correlate these parameters with arterial disease and symptoms as well as recovery. Earlier work has shown that computed tomography or MR imaging of intravascular (not freely diffusable) contrast agents cannot yet practically distinguish blood flow from blood volume (16) without the arterial input function, although relative cerebral blood volume can be reliably obtained. Figures 4 and 5 indicate that simple relative cerebral blood volume maps do not contain all the clinically relevant information available from the contrast injection in these patients.

This study was preliminary in nature. Additional studies in patients with acute stroke as well as chronic evolution of stroke would be helpful in further characterization of the mechanisms responsible for cortical dysfunction and recovery. In addition, it may be possible to use recently described techniques to map higher-order visual areas and use of higher-resolution techniques and other recent advances in functional MR (17, 18). Additionally, widespread clinical application of the simple techniques used here would be problematic. For example, activation mapping with functional MR relies on a selective stimulus. For primary visual cortex, full-field visual stimulation is straightforward and sufficient. Exploration of stroke affecting language or more than simple motor functions will require more complex paradigms. Another short-term barrier to functional MR is the severe demand on imaging hardware, analysis software, and computational resources. Importantly, two of our seven patients were unable to cooperate sufficiently to undergo full functional MR, which highlights yet another barrier to the application of these techniques. Nevertheless, these results have important implications for clinical and basic neuroscience applications. Combining traditional brain mapping techniques such as lesion studies with the in situ capability of functional MR to map the implications of lesions as demonstrated here will provide additional insight. Problems such as blindsight (19), defects in visual perception or cognition, and other questions regarding the hierarchical organization and functioning of the visual system now may be addressable in new ways. In addition, the combination of tissue hemodynamic mapping with functional MR and arterial mapping with MR angiography may provide a comprehensive evaluation of tissue at risk for secondary stroke; the true hemodynamic significance of upstream lesions may be assessable.

Conclusion

This study demonstrates in a preliminary way that functional MR can delimit abnormal function and hemodynamics after stroke. Abnormal function of brain tissue secondary to stoke can extend beyond the abnormalities seen on conventional imaging. Our data indicate hemodynamic abnormalities are detectable in stroke patients; further work is needed to determine whether such defects can be used as a clinical prognostic indicator. Both functional MR techniques used here may help assess the efficacy of therapeutic interventions. Finally, rehabilitation strategies may be improved by determining the areas of spared cortex that could be trained to take over the damaged tissues' tasks.

Acknowledgment

We thank T. Campbell for his expert technical assistance.

References

1. Horton JC, Hoyt WF. The representation of the visual field in human striate cortex. *Arch Opthalmol* 1991;109:816–824
2. Wolf PA, Belanger AJ, D'Agostino RB. Management of risk factors. *Neurol Clin* 1992;10:177–191
3. Cillessen JP, Kappell LJ, van Swieten JC, Algra A, van Gijn J. Does cerebral infarction after a previous warning occur in the same vascular territory? *Stroke* 1993;24:351–354
4. Fisher CM. Concerning the mechanism of recovery in stroke hemiplegia. *Can J Neurol Sci* 1992;19:57–63
5. Ogawa S, Lee TM, Nayak AS, Glynn P. Oxygenation-sensitive contrast in magnetic resonance image of rodent brain at high magnetic fields. *Magn Reson Med* 1990;14:68–78
6. Kwong K, Belliveau J, Chesler D, et al. Dynamic magnetic resonance imaging of human brain activity during primary sensory stimulation. *Proc Natl Acad Sci* 1992;89:5675–5679
7. Kent TA, Quast MJ, Kaplan BJ, et al. Cerebral blood volume in a rat model of ischemia by MR imaging at 4.7 T. *AJNR Am J Neuroradiol* 1989;10:335–338
8. Moseley ME, Kucharcyk J, Mintorovich J, et al. Diffusion-weighted MR imaging of acute stroke: correlation with T2-weighted and magnetic susceptibility-enhanced MR imaging in cats. *AJNR Am J Neuroradiol* 1990;11:423–429
9. Dixon W. Simple proton spectroscopic imaging. *Radiology* 1984; 153:189–194
10. Sepponen RE, Sipponen JT, Tanttu JI. A method of chemical shift imaging: demonstration of bone marrow with proton chemical shift imaging. *J Comp Assist Tomogr* 1984;8:585–587
11. Press W, Teukolsky S, Vetterling W, Flanner B. *Numerical Recipes in C: The Art of Scientific Computing*. 2nd ed. New York, NY: Cambridge University Press; 1992:
12. Belliveau J, Rosen B, Kantor H, et al. Functional cerebral imaging by susceptibility-contrast NMR. *Magn Reson Med* 1990;14:538–546
13. Starmer CF, Clark DO. Computer computations of cardiac output using the gamma function. *J Appl Physiol* 1970;28:219–220
14. Feeney DM, Baron J-C. Diaschisis. *Stroke* 1986;17:817–830
15. Conti DR. The stunned and hibernating myocardium: a brief review. *Clin Cardiol* 1991;14:708–712
16. Weisskoff R, Chesler D, Boxerman J, Rosen B. Pitfalls in MR measurement of tissue blood flow with intravascular tracers: which mean transit time? *Magn Reson Med* 1993;29:553–558
17. Schneider W, Noll DC, Cohen JD. Functional topographic mapping of the cortical ribbon in human vision with conventional MRI scanners. *Nature* 1993;365:150–153
18. Tootell R, Reppas J, Kwong K, et al. Functional analysis of human MT, and related visual cortical areas using magnetic resonance imaging. *J Neurosci* 1995;15:3215–3230
19. Fendrich R, Wessinger CM, Gassaniga MS. Residual vision in a scotoma: implications for blindsight. *Science* 1992;258:1489–1491